Emerging methods for the characterization of ischemic heart disease: ultrafast Doppler angiography, micro-CT, photon-counting CT, novel MRI and PET techniques, and artificial intelligence

Martin J. Willemink[1], Akos Varga-Szemes[2], U. Joseph Schoepf[2], Marina Codari[1], Koen Nieman[3,4], Dominik Fleischmann[1,4] and Domenico Mastrodicasa[1,4*]

Abstract

After an ischemic event, disruptive changes in the healthy myocardium may gradually develop and may ultimately turn into fibrotic scar. While these structural changes have been described by conventional imaging modalities mostly on a macroscopic scale—*i.e.*, late gadolinium enhancement at magnetic resonance imaging (MRI)—in recent years, novel imaging methods have shown the potential to unveil an even more detailed picture of the postischemic myocardial phenomena. These new methods may bring advances in the understanding of ischemic heart disease with potential major changes in the current clinical practice. In this review article, we provide an overview of the emerging methods for the non-invasive characterization of ischemic heart disease, including coronary ultrafast Doppler angiography, photon-counting computed tomography (CT), micro-CT (for preclinical studies), low-field and ultrahigh-field MRI, and ^{11}C-methionine positron emission tomography. In addition, we discuss new opportunities brought by artificial intelligence, while addressing promising future scenarios and the challenges for the application of artificial intelligence in the field of cardiac imaging.

Keywords: Artificial intelligence, Coronary artery disease, Myocardial infarction, Myocardial ischemia, Radiology

Key points

- Coronary ultrafast Doppler angiography detects the abnormal flow of postischemic intramural myocardial vessels.
- Photon-counting computed tomography (CT) allows for reduced radiation dose, increased spatial resolution, and differentiation between multiple contrast agents.
- Micro-CT combines functional cardiac imaging with myocardial metabolic assessment.
- Cardiac imaging has become feasible at low and ultrahigh-field MRI.
- ^{11}C-methionine positron emission tomography is used to characterize myocardial postinfarction inflammation.

* Correspondence: mastro@stanford.edu

This article is part of a thematic series on Myocardial tissue characterization in ischemic heart disease (Guest Editors: Akos Varga-Szemes and Pal Suranyi, MUSC Health Charleston, SC, United States).

[1]Department of Radiology, Stanford University School of Medicine, 300 Pasteur Drive, Stanford, CA 94035, USA

[4]Stanford Cardiovascular Institute, Stanford, CA 94305, USA

Full list of author information is available at the end of the article

Background

Ischemic heart disease (IHD) is the leading cause of death globally [1, 2]. The assessment of myocardial ischemic changes is crucial to diagnose IHD accurately, to

estimate patients' prognosis, and therefore to evaluate optimal therapeutic options [3]. Traditionally, stress echocardiography and invasive angiography have been valuable means for IHD diagnosis and treatment, respectively [4–6]. Cardiovascular computed tomography (CT) and magnetic resonance imaging (MRI) provide sophisticated and complementary information through an exceptional high-quality visualization of coronary arteries, as well as of the cardiac structures and function. In addition, nuclear medicine imaging is a well-established tool for the non-invasive assessment of myocardial perfusion in patients with suspected IHD. Extensive research has described the strengths and weaknesses of these conventional imaging modalities [7–9]. Recently, novel imaging methods have shown the potential to unveil a highly detailed picture of the postischemic myocardial phenomena, which may lead to a more comprehensive evaluation of IHD [10, 11]. There is evidence suggesting these new methods may bring pivotal advances in the understanding of IHD, with potential major changes in the current clinical practice.

In this review article, we provide an overview of the emerging methods and tools for the noninvasive characterization of the ischemic myocardial tissue (Fig. 1). We considered techniques used in both the clinical and preclinical setting, including ultrafast cardiac ultrasound, x-ray-based technologies (micro-CT and photon-counting CT), molecular imaging, and low- and ultrahigh-field MRI. Finally, we provide a brief update on the most recent applications of artificial intelligence (AI) in the field of cardiac imaging.

Ultrafast ultrasound

Coronary microvascular dysfunction is considered an important prognostic marker for myocardial ischemia [12, 13]. However, the *in vivo* assessment of the human coronary tree has been limited mostly to the epicardial
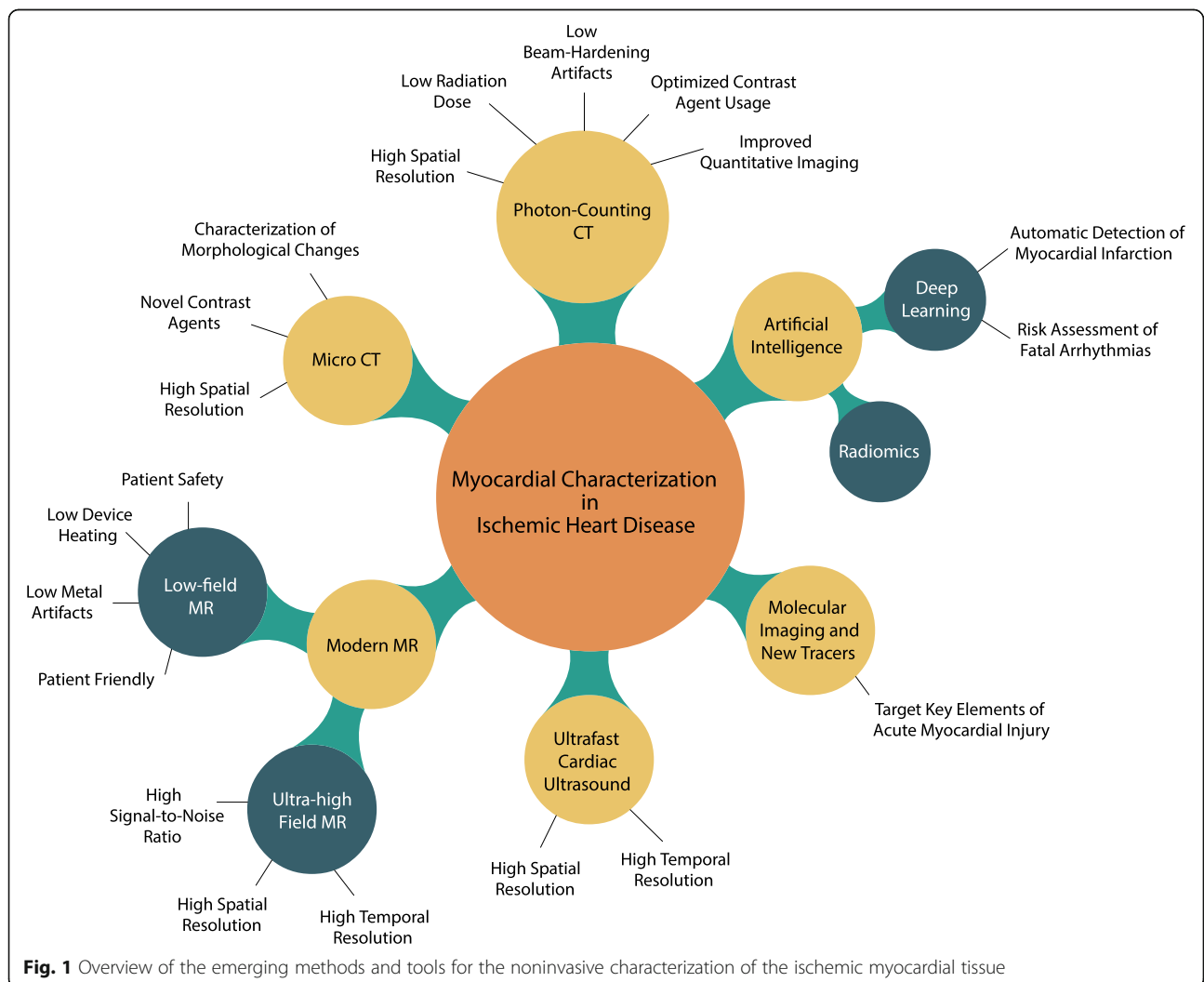

Fig. 1 Overview of the emerging methods and tools for the noninvasive characterization of the ischemic myocardial tissue

vasculature, thus leaving the intramural vessels largely unexplored. The most recent technological advancements in echocardiographic imaging allow to image the heart at a pace 100 times faster than conventional echocardiography, with higher spatial and temporal resolution [14]. This novel imaging approach, known as ultrafast cardiac ultrasound, has been tested in the preclinical arena and has shown the potential to unveil new information in areas of myocardial mechanics and vascular flow analysis mostly unexplored so far. Recently, Maresca et al. [10] reported the use of cardiac ultrafast ultrasound in combination with adaptive coronary Doppler processing to visualize epicardial and intramural coronary vessels. The authors conducted a series of open-chest experiments on nine swine models using a new technique they named coronary ultrafast Doppler angiography (CUDA). In their experiment, the authors determined coronary flow changes after a brief (30 s) occlusion of the left anterior descending artery followed by reperfusion, to study the hyperemia occurring in the anterior wall of the left ventricle. In addition, the authors obtained noninvasively the coronary flow reserve after the intravenous administration of adenosine. A left anterior descending artery flowmeter probe was used to validate their findings. Later, the left anterior descending artery occlusion was prolonged to 90 min to induce myocardial infarction and documented abnormal arterial and venous flow. Interestingly, in an effort to translate this technology into clinical practice, CUDA was initially tested on four healthy human volunteers, two adults and two pediatric patients, only for the visualization of the coronary vasculature (Fig. 2). Both arterial and venous intramural vessels were detected in a beating heart, though at the cost of a lower image spatial resolution due to the traditional transthoracic approach.

As radiation and contrast-free imaging modality, CUDA is a promising tool in the field of myocardial injury characterization. More so, if we consider its ability to assess coronary flow reserve noninvasively, which would be paramount in patients with stable coronary disease. However, there are still critical hurdles to its clinical implementation. CUDA is based on the use of a linear transducer array that extends the imaging depth to a maximum of 45 mm, a distance that is unfit for the majority of adult patients. Moreover, CUDA was unable to provide an absolute quantification of the flow rate. Nonetheless, CUDA provided a solid foundation for *in vivo* imaging of intramural coronary vessels and coronary blood flow variations.

Micro-CT

Micro-CT is a well-established preclinical research tool, because of its high spatial resolution and the opportunity to characterize morphological changes in anatomical structures approaching the micrometer range. Moreover, modern micro-CT scanners are equipped with advanced cardiorespiratory gating and are able to acquire four-dimensional datasets [15], therefore providing an accurate assessment of the cardiac function (Fig. 3). Both *in vivo* and *ex vivo* small animal studies have been used as models for human cardiovascular conditions, ranging from atherosclerosis [17–21] to congenital heart defects [22, 23] to enhance the understanding of diseases and develop potential targeted therapies. Sangaralingham et al. [22] investigated the aging coronary vasculature in Fischer rats. They found that micro-CT was able to detect the reduction in intramyocardial vessel volume in the aged heart along with increased epicardial vessel volume, left ventricular fibrosis, and mild dysfunction. Pai et al. [19] demonstrated that micro-CT could also be used for vessel wall imaging of the coronary arteries in mice. The authors used osmium tetraoxide as a tissue-staining contrast agent that is retained in the vessel wall and reported that coronary arteries as small as 45 μm in diameter can be visualized. While micro-CT has been proven to be able to acquire isotropic data on cardiac morphology and function, it also has the advantage of being faster than MRI, therefore providing high-resolution image data, even under dobutamine-induced stress, as demonstrated by Badea et al. in healthy adult rats [24].

Due to the increased spatial resolution of micro-CT and consequent possibility to visualize microstructures and metabolic processes, novel contrast agents had to be developed to provide tissue differentiation on the microscopic level. Ashton et al. [25] investigated the preclinical use of eXIA 160, an aqueous colloidal polydisperse contrast agent with a high iodine concentration taken up by the myocardium and other metabolically active tissues. More specifically, they demonstrated the potential role of eXIA 160 for imaging myocardial infarction in mice: immediately after eXIA 160 intravenous administration, an about 340 HU signal density difference between blood and myocardium allowed for ventricular volumetry and function assessment. In addition, the about 140 HU contrast difference between normal and infarcted myocardium four hours after the injection enabled quantification of infarct size using dual-energy micro-CT, validated against micro-single-photon emission computed tomography and *ex vivo* histopathology. Van Deel et al. [26] demonstrated similar results using the same contrast agent in micro-CT studies for the assessment of global and regional myocardial function, myocardial perfusion, metabolism, and viability in a mouse model of myocardial ischemia induced by permanent occlusion of the left anterior descending coronary artery.

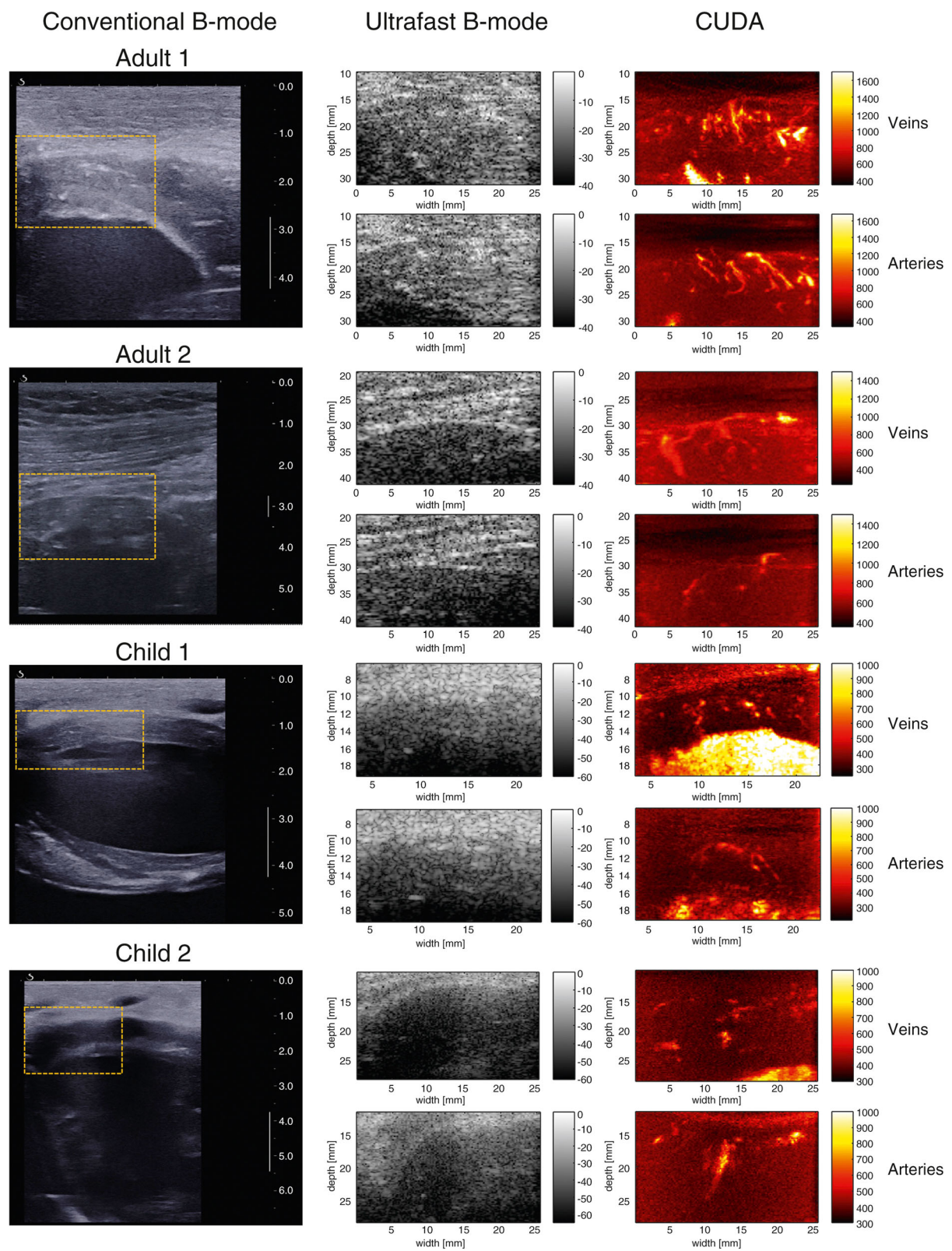Among the other innovative contrast agents, ExiTron MyoC 8000, a nanoparticulate agent, was optimized for

Fig. 2 (See legend on next page.)

(See figure on previous page.)
Fig. 2 Left: conventional ultrasound image showing the region of interest selected for coronary ultrafast Doppler angiography (CUDA) processing. This real-time imaging mode of the ultrasound scanner was used for positioning (the scale bar is in centimeters). Middle: ultrafast B-mode images of the region of interest depicted in yellow on the images in the left column. Right: CUDA images of coronary veins in systole and coronary arteries in diastole. (Reprinted, with permission, from [10])

CT studies of the myocardium. It is composed of a polymer shell and a liquid core, with a mean hydrodynamic diameter of about 300 nm, showing ultrahigh density values (about 8,000 UH). Its accumulation in the healthy myocardial tissue combine with its long blood half-life (about 2 h in mice) allows for visualizing myocardial pathological changes as well to perform functional cardiac imaging [27]. This agent has been tested in micro-CT to longitudinally monitor cardiac processes *in vivo*, in mice with myocardial infarction [28]. ExiTron MyoC 8000-enhanced micro-CT imaging was able to detect and accurately quantify myocardial infarction, even at a very low contrast dose (50 μL per 25-g mouse body weight, 210 mg I/mL).

The main limitation of micro-CT is the size of the CT tube that is able to accommodate small animals only. While less relevant to animal studies, the substantial radiation exposure will pose further challenges when human studies will be considered.

Photon-counting CT

CT is a remarkably successful technology, which is reflected in the increasing number of exams performed annually [27]. Despite its success, CT has important limitations including (1) relatively high x-ray radiation exposure, (2) limited soft tissue differentiation, and (3) use

Fig. 3 Axial and coronal views of systole and end-diastole in a mouse model with intravascular iodine contrast. Projection data were sampled using a prospective gating scheme. These images represent two of the ten cardiac acquired phases, *i.e.*, diastole and systole. Reconstruction was performed using a four-dimensional iterative technique based on the split Bregman method [16]. Figure courtesy of Dr. Cristian T. Badea, PhD, Duke University

of iodinated contrast agents [11]. Some of these issues can theoretically be solved by dual-energy CT, which provides iodine concentration maps and material-specific images. Separation between high-energy and low-energy x-ray photons (the so-called spectral separation) is, however, suboptimal with current dual-energy CT systems [29]. A more robust solution that has the potential to address current technical CT limitations is photon-counting CT. Despite the fact that photon-counting CT is currently not yet commercially available, it is expected that this technique will dramatically change CT imaging [11].

The improved noise behavior of photon-counting detectors may allow for reduced radiation exposure. This is relevant for cardiovascular imaging since, despite major improvements over the last decades, radiation doses are still substantial for cardiovascular imaging protocols [30]. Symons et al. [31] assessed the performance of photon-counting CT for coronary artery calcium quantification in 10 *ex vivo* hearts and 10 asymptomatic volunteers without electrocardiography gating. Their results indicated that either image quality of coronary artery calcium scans can be achieved or radiation dose can be reduced with photon-counting CT. Kappler et al. [32] assessed water phantoms and found increased attenuation of iodine with comparable image noise as conventional energy-integrating detectors. The increased contrast-to-noise ratios may allow for a reduction in radiation dose of up to 32%, as confirmed by recent investigations conducted in the field of brain [33] and chest imaging [34].

Smaller detector elements typical of photon-counting CT scanners may allow for improved spatial resolution. Currently, assessment of coronary stenoses is substantially limited in the presence of calcium or stents due to blooming artifacts. Since blooming is dependent on the point-spread function of the CT system, the increased spatial resolution of photon-counting detectors may result in less blooming [35]. Multiple recent studies have evaluated the utility of high spatial resolution photon-counting CT for cardiovascular applications. Symons et al. [36] conducted a phantom study with 18 coronary stents with diameters ranging from 2.0 to 4.0 mm and found significantly improved visibility of the coronary stent lumen. Similarly, Mannil et al. [37] assessed 18 coronary stents with a diameter of 3.0 mm with luminal iodinated contrast and found superior in-stent lumen
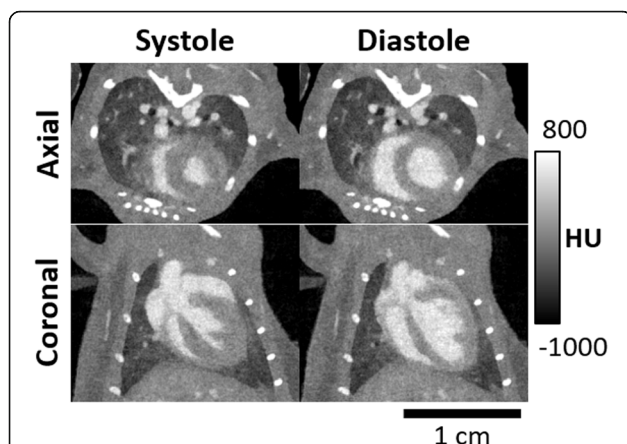
Willemink *et al. European Radiology Experimental* (2021) 5:12

Page 6 of 14

delineation compared with conventional energy-integrating detectors.

Beam-hardening artifacts can be corrected for due to improved material decomposition. Beam-hardening artifacts caused by surrounding anatomical structures or implanted devices hamper the evaluation of myocardial perfusion. Decreased beam-hardening artifacts may thus enhance the performance of myocardial perfusion CT. Symons et al. [38] acquired photon-counting CT angiography exams of the head and neck region in 16 volunteers with a 140-kV tube voltage. All volunteers also underwent a 120-kV exam with a conventional CT system at a comparable radiation dose. Despite the higher tube voltage, contrast-to-noise ratios were similar, and most importantly, beam-hardening artifacts were less severe in the photon-counting CT exams. Using the high-energy portion of photon-counting detector data can also reduce beam-hardening artifacts. A study conducted by Pourmorteza et al. [33] in 21 asymptomatic volunteers suggested that high-energy photons were less affected by beam hardening. The disadvantage is that this approach results in reduced tissue contrast.

The use of contrast agents may be optimized with photon-counting CT. Patients who are allergic to iodine or patients with decreased kidney function would benefit from CT image acquisition with reduced iodine concentrations or other contrast agents, such as gadolinium. Since photon-counting CT has the potential to improve contrast-to-noise ratio, not only radiation dose can potentially be decreased, also iodine contrast concentrations may be reduced. A variety of studies has shown improved contrast-to-noise ratio with photon-counting CT compared with conventional energy-integrating detectors. Yu et al. [39] showed in a phantom study that the contrast-to-noise ratio of iodine *versus* water increased by up to 25.5%, which may allow for iodine contrast load reduction. Besides iodine load reduction, alternative contrast agents, either through systemic or targeted administration, may also be considered with photon-counting CT, such as gadolinium, barium, gold, and platinum. Cormode et al. [40] scanned apolipoprotein E knockout mice on a photon-counting CT system after injecting gold nanoparticles and iodine. They concluded that valuable information might be yielded about atherosclerotic plaque composition. This indicates that photon-counting CT allows for differentiation between simultaneously administered multiple contrast agents, and the specific distribution of these contrast agents may result in additional information. Symons et al. [41] intravenously administered gadolinium and iodine and orally administered bismuth in an occlusion-reperfusion canine model of myocardial infarction. This study showed that concentrations of these contrast agents, as well as the wash-in wash-out kinetics, could be quantified.

Photon-counting CT offers the opportunity to improve quantitative imaging compared with current CT technology. Materials and tissues can be differentiated with color-coded images that are material/tissue specific. Not only can different materials be displayed, but also concentrations of materials, such as contrast agents and calcium, can be quantified, independent of acquisition settings. Quantification of material concentration may benefit myocardial perfusion analyses since this allows for the exact concentration determination of contrast agents in the myocardium. Moreover, coronary calcium is currently quantified with the Agatston score [42], which is dependent on acquisition parameters such as tube voltage and reconstruction parameters such as slice thickness. Quantification of calcium with photon-counting CT is independent of these parameters and may thus allow for the exact quantification of coronary calcium mass. Another advantage may be a more precise quantification due to reduced blooming artifacts.

Unfortunately, the ideal photon-counting CT system does not exist yet. Currently, only prototype systems are in development for human-sized imaging. It is expected that the first commercial photon-counting CT scanners for humans will become available within the next 3 to 10 years. Before clinical implementation, important challenges need to be tackled. *Cross-talk* is still a problem with current photon-counting detectors [43]. Despite reduced cross-talk compared with conventional energy-integrating detectors, x-ray photons may hit the detector right on the border between two detector elements. Also, part of the energy may be released in the form of fluorescence photons, which may move to a random location, potentially a neighboring detector element, resulting in cross talk. Many incoming x-ray photons hit CT detectors in a short time [44]. To be able to count every photon separately, a fast detector is required. Pileup of x-ray photons is currently still a problem with photon-counting detectors. Since x-ray photon count rates are lower in micro-CT imaging, photon-counting detectors are also evaluated for micro-CT [45]. Up to our knowledge, there are currently no photon-counting CT systems available that allow for electrocardiography synchronization, which is necessary for myocardial infarction assessment of CT images. However, it is expected that electrocardiography synchronization will be enabled on photon-counting CT in the short term.

Molecular imaging and new tracers
Myocardial infarction and the subsequent reperfusion of the infarcted myocardial tissue ignite a complex series of biological events culminating in the development of a fibrotic scar [46]. The detailed characterization of these

phenomena represents a challenging task for imaging modalities commonly used in clinical practice since these techniques currently tend to focus more on the macroscopic anatomical and functional aspects of the heart. In the last few decades, new positron emission tomography (PET) tracers and MRI agents have been developed to target key elements of acute myocardial injury, defined by cardiomyocyte death and endothelial damage, and chronic cardiac remodeling. For instance, Sosnovik et al. [47] targeted Annexin-V, a marker expressed in apoptotic cells, to characterize acute ischemia and heart failure in mice. Imaging targets sensitive to vascular permeability have been tested as well. A family of cell-surface proteins known as integrins are considered a marker of angiogenic vascular tissue. $A_v\beta_3$ is an integrin whose expression is abundant in newly formed blood vessels, which is a process associated with endothelial damage [48]. Arginyl-glycyl-aspartic acid (RGD) is a short peptide sequence recognized by integrins, and it is expressed on extracellular matrix proteins and membrane surfaces. Several preclinical and clinical studies showed that RGD-based radiotracers labeled with fluorine and gallium were able to document the angiogenesis occurring in the regeneration process following myocardial infarction [49, 50]. Notably, only ^{18}F-galacto-RGD has been described in patients with myocardial infarction [49]. Recently, Lavin et al. [51] developed a new gadolinium-based albumin-binding contrast agent, gadofosveset, and demonstrated the feasibility of imaging vascular permeability in a murine model of myocardial infarction.

Another key process of the postinfarction cardiac remodeling is the deposition of new extracellular matrix, typically rich in collagen and elastin. Elastin can preserve elasticity in the infarcted regions, thus leading to an improved ejection fraction [52]. As such, elastin represents an interesting remodeling biomarker, along with its precursor tropoelastin. Elastin/tropoelastin-specific MRI contrast agents have been used to assess the extracellular matrix remodeling in preclinical studies [53–55].

Monocytes and leukocytes are among the several immune cells generating an inflammatory response within the ischemic myocardium. These cells have been targeted to characterize the myocardial inflammation occurring after an ischemic insult. For instance, ^{18}F-fluorodeoxyglucose (FDG), a tracer well-known in the field of cancer imaging, has been used in association with PET-CT to characterize the metabolic activity of the infarcted myocardium. The infarcted myocardium is, in fact, rich in leukocytes [56], which have an elevated metabolic activity. However, the FDG uptake by viable cardiac cells represents a confounding factor. To suppress the signal from normal cardiac cells, patients have to follow specific dietary restrictions [57]. The results

tend to be suboptimal, and therefore, more specific tracers are warranted. ^{18}F-fluorodeoxymannose is a potential alternative, based on a glucose isomer (mannose), suggested for imaging of macrophages [58]. So far, its applications have been limited to preclinical studies.

Macrophages have also been targeted using ^{68}Ga-DOTATATE and ^{68}Ga-DOTATOC, two radiotracers with an affinity for the somatostatin receptors types 2 and 5, respectively, expressed in macrophages [57–60]. ^{68}Ga-pentixafor is a PET radiotracer targeting the chemokine receptor CXCR4, which is thought to play a role in leukocyte recruitment to the injured myocardial tissue. ^{68}Ga-pentixafor has been used in mice and translated to patients to highlight the expression of CXCR4 during the early inflammatory state occurring after myocardial infarction [61, 62]. Interestingly, the expression of CXCR4 was more heterogeneous in patients, suggesting a unique and complex clinical environment for each patient, which could have important implications in patients' prognosis and therapy.

[11]C-methionine is a clinically approved agent, known mostly in the oncologic field, which accumulates in macrophages [63]. Therefore, it represents an ideal imaging target to characterize postinfarction myocardial inflammation. A PET study using ^{11}C-methionine demonstrated a high signal in the early stages of myocardial infarction, declining seven days from the ischemic insult [64]. The peculiar temporal window of ^{11}C-methionine indicates an accurate characterization of the early stages of myocardial infarction and, therefore, with important implications for the assessment and efficacy of targeted therapies.

Although most of the above-described studies are preclinical, they are immensely relevant because they showed the potential to provide more detailed information on IHD, therefore leading to a more tailored patient management and optimized therapies. More research is needed to validate these new options in large clinical populations.

Low-field and ultrahigh-field MRI

Cardiac MRI has the advantage to provide high soft tissue contrast and therefore differentiation of various tissue entities within the myocardium. Moreover, it has the ability to evaluate function, perfusion, and flow in addition to structure. While the standard MRI field most commonly used for cardiac applications is 1.5 T, there are certain benefits, and also shortcomings, of moving towards the lower or upper end of the currently achievable magnetic field range as detailed below.
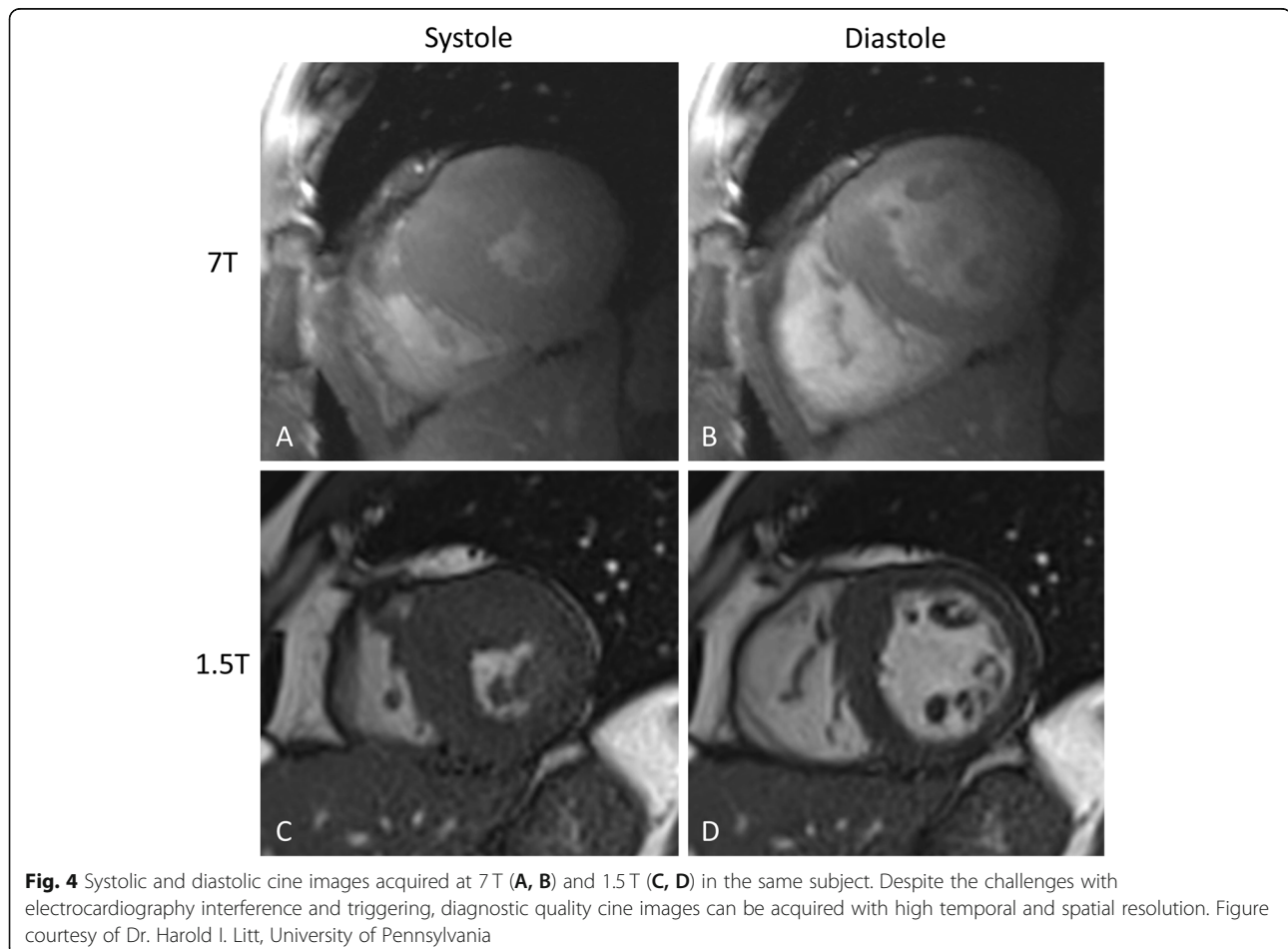
Low-field MRI (≤ 0.35 T) has been around for decades and we now see the revamp in the utilization of this technique again due to technology improvements allowing for cardiac imaging at such a low-field range. As

recently demonstrated by Simonetti and Ahmad [65], low-field MRI has the advantage of improved patient safety (low ferromagnetic attraction, practically no specific absorption rate limits), reduced device heating and artifacts related to metallic implants, reduced equipment and maintenance cost, and more patient-friendly design since the bore of the low-field magnets can be configured as open MRI systems. Such low-field applications may be beneficial in patients with *de novo* implants when MRI is usually not recommended during the first two weeks. While low-field MRI comes with the disadvantage of low signal-to-noise ratio, Simonetti and Ahmad reported promising results with cine, phase-contrast, and black blood cardiac imaging, using advanced image reconstruction techniques, such as Sparsity Adaptive Compressive Recovery (SCoRe) [65], which allows for adequate image quality to generate diagnostic images. The further potential advantages of low-field MRI are the lower equipment and operational costs and the improved simplicity of image acquisition.

As MRI technology advances towards the direction of higher field strengths as seen recently by the increasing number of 7-T whole body systems installed in multiple

academic institutions, it is important to assess what advantages can be gained for IHD assessment by such high field and what drawbacks we are facing. A clear benefit of 7-T systems is the exceptional signal-to-noise ratio as well as increase in spatial and temporal resolution [66]. The limitations, however, are substantial, especially for cardiovascular imaging [67, 68]: increased heating of metal implants, increased ferromagnetic attraction, increased field inhomogeneity, more prominent electrocardiography interference caused by magneto-hydrodynamic effects [69] and increased metallic device-related artifacts [65]. A 7-T image example is shown in Fig. 4.

Despite these limitations, recent literature demonstrates that the use of 7-T systems, either as small bore for experimental research or large bore for human applications, has potential in certain fields of cardiovascular imaging. Zhang et al. [70] investigated and found T2 mapping feasible and reliable at 7 T to characterize myocardium in order to quantify the area at risk, infarct core, intramyocardial hemorrhage, and salvaged myocardial zone in a rat model of myocardial infarction. Spath et al. [71] tested the application of manganese-enhanced

Fig. 4 Systolic and diastolic cine images acquired at 7 T (**A, B**) and 1.5 T (**C, D**) in the same subject. Despite the challenges with electrocardiography interference and triggering, diagnostic quality cine images can be acquired with high temporal and spatial resolution. Figure courtesy of Dr. Harold I. Litt, University of Pennsylvania

MRI in a rat model of myocardial infarction. They found that manganese-enhanced MRI causes calcium channel-dependent myocardial T1 shortening, and T1 mapping was able to provide an accurate assessment of infarct size and changes in calcium handling in the remote myocardium, which may hold potential for the assessment of myocardial viability, remodeling, and regeneration. Myocardial infarction in a rat model has also been studied using Gadofluorine P in a combined MRI and mass spectrometry approach [72]. Wang et al. [73] demonstrated that late gadolinium enhancement imaging can be performed at 7 T in a rat model of myocardial infarction in a self-gated fashion, *i.e.,* without electrocardiography and respiratory gating.

Promising approaches have been proposed for 7-T human cardiac imaging as well. An acoustic cardiac triggering technique has been introduced by Frauenrath et al. [74] for synchronization and gating of cardiac MRI studies at 7 T, which has been demonstrated to have superior reliability and fidelity compared with that of conventional vector electrocardiography and traditional pulse oximetry. Acoustic cardiac gating is based on the phonocardiogram signal, and uses the first heart tone for acquisition triggering. von Knobelsdorff-Brenkenhoff et al. [75] studied fast gradient-echo imaging for cardiac chamber volume quantification at 7 T in nine subjects, and found it feasible and in good agreement with balanced steady-state free precession-based measurements in the same subjects at 1.5 T. Hezel et al. [76] investigated the feasibility of human myocardial mapping at 7-T ultrahigh field and found that challenges, such as signal voids, can be addressed by using tailored shimming techniques and dedicated acquisition schemes. Prothmann et al. [77] performed late gadolinium enhancement imaging in 131 patients at 7 T and found the technique feasible to detect myocardial fibrosis with higher spatial resolution compared to 3 T.

While most of these studies aimed to establish feasible techniques for 7-T cardiac imaging, an increasing effort in the scientific community to explore the potentials of ultrahigh-field MRI can clearly be recognized.

Overall, new MRI techniques may potentially improve access to MRI due to the lower cost and improved patient compliance at low field, and open up new avenues in the characterization of the ischemic myocardium by employing the single-to-advantages of high-field imaging.

AI applications in cardiac imaging

In light of the advent of *big data*, along with the availability of powerful computational technology, AI applications are thriving in the field of medical imaging at an unprecedented pace [78, 79]. This holds true for cardiac imaging, where recent studies have shown preliminary,

but promising results that may take cardiac imaging further than ever. Among AI algorithms, deep learning (DL) has been successfully applied, ranging from image reconstruction and denoising, to image classification, segmentation, and interpretation [80–83].

Since "upstream" AI applications, such as image reconstruction and denoising, are more general and not specifically related to IHD diagnosis, in this review, we will focus on "downstream" AI applications specifically related to the topic at issue [84].

For instance, Zreik et al. [85] identified patients with hemodynamically significant coronary stenoses relying solely on the automatic analysis of the left ventricular myocardium on rest coronary CT angiography (CCTA) scans. To this end, the authors used a convolutional neural network to segment the left ventricle myocardium, an unsupervised convolutional autoencoder to extract myocardial features and machine learning classifier to analyze CCTA data. The proposed pipeline reached an average area under the curve (AUC) at receiving operator characteristic analysis of 0.74 ± 0.02 (mean ± SD) during10-fold cross-validation performed in 126 scans. This method was then applied by van Hamersvelt et al. [86] in 101 patients with intermediate coronary stenosis to evaluate the impact of an additional DL-based analysis of the myocardium to identify those with functionally significant stenosis. They reported an improvement in AUC values when the DL approach was combined with the determination of the coronary degree of stenosis against the coronary degree of stenosis alone (0.76 *versus* 0.68). Moreover, though the DL analyses were focused on the myocardium only, the visual assessment of coronary arteries improved also the sensitivity. These studies further confirmed the potential of CCTA as the ultimate gatekeeper for unnecessary invasive angiography studies. Future automated approaches will probably benefit from a more complete evaluation coupling the left ventricular myocardium analysis with computational fluid dynamics applied to the coronary tree.

By using a recurrent neural network, Xu et al. [87] were able to automatically detect areas of myocardial infarction on cardiac MRI scans with an overall pixel classification accuracy of 94.4% in a sample of 114 subjects. This end-to-end DL framework enabled the accurate detection of the infarction size at the pixel level, which has the potential to reduce the inter-observer variability of the visual assessment of late gadolinium enhancement and therefore improve the efficiency in myocardial infarction diagnosis even in less experienced readers.

When LGE imaging cannot be performed due to contraindications to gadolinium-based contrast agents, a non-contrast approach would be highly desirable. Zhang et al. [88] introduced a DL framework to diagnose chronic myocardial infarction in 212 patients using

unenhanced cardiac cine MRI images. Their approach allowed to identify chronic myocardial infarction in testing data with sensitivity of 0.90 a specificity of 0.99, and an AUC of 0.94. Based on extracted motion features, the authors proved that it is possible to determine the presence, location, size, and degree of transmural extent of the myocardial infarction without the need for gadolinium-based contrast agent injection.

Radiomics is another promising approach with the potential to expand our knowledge of information contained in cardiovascular digital images and to realize a step forward toward precision medicine [89]. Radiomics is essentially a process enabling the extraction of a large number of handcrafted or DL-based quantitative features from selected areas in radiological images. These features could also be used to identify meaningful associations with clinical or outcome data, thus providing novel imaging biomarkers [90]. Radiomics has been quite successful in oncology [91, 92]; however, the experience in cardiovascular imaging is limited. Recently, few studies demonstrated the feasibility and potential clinical value of radiomics analysis in cardiac CT and MRI images.

In a proof-of-concept study, Mannil et al. [93] tested radiomic features and six machine learning-based classifiers to detect myocardial infarction on unenhanced, low-radiation dose cardiac CT images of 57 patients with acute and chronic myocardial infarction and 30 controls. The authors were able to distinguish controls and patients with acute or chronic myocardial infarction with an AUC value of 0.78. This study was inspired by a previous investigation by Baessler et al. [94], who showed the potential of texture analysis in enabling the

automatic diagnosis of small and large myocardial infarction on unenhanced cardiac cine MRI reaching AUC value of 0.92.

Similar studies by Larroza et al. [95] applied radiomics to discriminate nonviable, viable, and remote segments in unenhanced cine MRI scans of 50 patients. Among developed support vector machine classifiers, the best one showed AUC values on testing data equal to 0.935, 0.819, and 0.794 for nonviable, viable, and remote segments, respectively. The same group previously reported a radiomic analysis on late gadolinium cardiac MRI of 44 subjects that allowed to distinguish acute from chronic myocardial infarction with an AUC of 0.86 ± 0.06 (mean $\pm$ SD) during nested cross-validation [96].

Radiomics has also been reported to predict relevant clinical outcomes, such as post-myocardial infarction arrhythmias. Kotu et al. [97] investigated 34 patients with chronic myocardial infarction and performed a radiomic analysis of the myocardial scar. With this approach, they were able to identify patients with a high-risk of developing post-myocardial infarction fatal arrhythmias with an average AUC of 0.92 during a nested cross-validation.

These investigations (Table 1) are the foundational evidence that AI can be used in cardiovascular imaging to overcome the limits of a purely visual image assessment and provide a more complete evaluation, even in patients where late gadolinium enhancement imaging is not feasible. More AI-based applications are being developed in other areas of cardiovascular imaging; however, such applications go beyond the scope of this paper and have been extensively discussed [79, 90, 98–100].

Table 1 Artificial intelligence applications in ischemic heart disease

Authors (year) [reference]	AI approach	Imaging modality	Description
Zreik et al (2018) [85]	Deep learning	CT	Significant coronary stenosis detection based on left ventricular myocardium analysis
van Hamersvelt et al (2019) [86]	Deep learning	CT	Significant coronary stenosis detection based on left ventricular myocardium analysis in patients with intermediate stenosis
Xu et al (2017) [87]	Deep learning	MRI	Myocardial infarction size automatic detection
Zhang et al (2019) [88]	Deep learning	MRI	Chronic myocardial infarction diagnosis based on non-contrast cardiac cine MRI
Mannil et al (2018) [93]	Deep learning and radiomics	CT	Myocardial infarction detection based on non-contrast cardiac CT
Baessler et al (2018) [94]	Radiomics	MRI	Subacute and chronic myocardial infarction detection on non-contrast cardiac CT
Larroza et al (2018) [95]	Radiomics	MRI	Distinction between nonviable, viable, and remote segments on enhanced cine MRI
Larroza et al (2017) [96]	Radiomics	MRI	Acute and chronic myocardial infarction distinction based on cine and LGE cardiac MRI
Kotu et al (2015) [97]	Radiomics	MRI	Fatal arrhythmias risk assessment based on myocardial scar analysis from LGE cardiac MRI

AI Artificial intelligence, *CT* Computed tomography, *LGE* Late gadolinium enhancement, *MRI* Magnetic resonance imaging

Despite the promising initial results, there are concerns regarding the translation of AI-based tools into clinical practice. One of the main hurdles is the lack of a clear explanation of how these algorithms work. AI relies on machine learning and deep learning algorithms whose complexity makes them essentially a "black-box" system. The lack of transparency and explainability could result in limited trust and therefore, restricted use of AI in healthcare [101]. A similar effect could be caused by the input data used to train the algorithms, which should be as representative as possible of the population they are going to serve. The challenge of the next wave of AI will be to use more transparent algorithms and apply those algorithms to a larger scale, which most likely implies the collaboration of multiple centers around the world.

Future outlook

As we reported in this review article, a variety of technological developments in cardiac imaging is expected to open new avenues in more advanced visualization, quantification, and prognostication of IHD. The potential new techniques, such as photon-counting CT, and low- and ultrahigh-field MRI, may bring major changes in our current clinical imaging practice. In combination with AI-based approaches, our imaging strategies, analysis approaches, and overall efficiency may see such substantial improvements that we have not seen for years in radiology.

Abbreviations
AI: Artificial intelligence; AUC: Area under the curve; CCTA: Coronary computed tomography angiography; CT: Computed tomography; CUDA: Coronary ultrafast Doppler angiography; DL: Deep learning; IHD: Ischemic heart disease; MRI: Magnetic resonance imaging; PET: Positron emission tomography; RGD: Arginyl-glycyl-aspartic acid

Authors' contributions
All authors drafted the article and revised it critically for important intellectual content. All authors gave final approval of the version to be submitted and any revised version.

Competing interests
MJW: Activities related to the present article: none. Activities not related to the present article: research grants from American Heart Association (18POST34030192), Philips Healthcare, and Stanford University, consulting for Arterys, Inc, and co-founder/shareholder of Segmed, Inc. Other relationships: disclosed no relevant relationships.
AVS receives institutional research support and/or personal fees from Elucid Bioimaging and Siemens. AVS is one of the Guest Editors of this thematic series. The paper was therefore reviewed and handled by the *European Radiology Experimental* Editor-in-Chief Prof. Francesco Sardanelli and the Guest Editor Prof. Pal Suranyi.
UJS receives institutional research support and/or personal fees from Astellas, Bayer, Bracco, Elucid Bioimaging, Guerbet, HeartFlow, and Siemens.
KN received institutional research support from Siemens Healthineers, Bayer healthcare, GE Healthcare, and Heartflow Inc.
DF: Activities related to the present article: none. Activities not related to the present article: received research support from Siemens Healthineers and GE Healthcare; is on the Speakers' Bureau at Siemens Healthineers; has ownership interest in iSchemaView. Other relationships: disclosed no relevant relationships. The other authors have no conflict of interest to disclose.

Author details
[1]Department of Radiology, Stanford University School of Medicine, 300 Pasteur Drive, Stanford, CA 94035, USA. [2]Division of Cardiovascular Imaging, Department of Radiology and Radiological Science, Medical University of South Carolina, Charleston, SC, USA. [3]Division of Cardiovascular Medicine, Stanford University School of Medicine, Stanford, CA, USA. [4]Stanford Cardiovascular Institute, Stanford, CA 94305, USA.

References
1. Nowbar AN, Gitto M, Howard JP, Francis DP, Al-Lamee R (2019) Mortality from ischemic heart disease. Circ Cardiovasc Qual Outcomes 12:e005375 https://doi.org/10.1161/CIRCOUTCOMES.118.005375
2. GBD 2017 Causes of Death Collaborators (2018) Global, regional, and national age-sex-specific mortality for 282 causes of death in 195 countries and territories, 1980-2017: a systematic analysis for the Global Burden of Disease Study 2017. Lancet 392:1736-1788 https://doi.org/10.1016/S0140-6736(18)32203-7
3. Knuuti J, Wijns W, Saraste A et al (2020) 2019 ESC Guidelines for the diagnosis and management of chronic coronary syndromes. Eur Heart J 41: 407–477 https://doi.org/10.1093/eurheartj/ehz425
4. Pellikka PA, Arruda-Olson A, Chaudhry FA et al (2020) Guidelines for performance, interpretation, and application of stress echocardiography in ischemic heart disease: from the American Society of Echocardiography. J Am Soc Echocardiogr 33:e48 https://doi.org/10.1016/j.echo.2019.07.001
5. Maron DJ, Hochman JS, Reynolds HR et al (2020) Initial Iivasive or conservative strategy for stable coronary disease. N Engl J Med 382:1395–1407 https://doi.org/10.1056/NEJMoa1915922
6. Pellikka PA, Nagueh SF, Elhendy AA, Kuehl CA, Sawada SG, American Society of Echocardiography (2007) American Society of Echocardiography recommendations for performance, interpretation, and application of stress echocardiography. J Am Soc Echocardiogr 20:1021–1041 https://doi.org/10.1016/j.echo.2007.07.003
7. Gibbons RJ, Carryer D, Hodge D, Miller TD, Roger VL, Askew JW (2020) Stress testing in the evaluation of stable chest pain in a community population. Mayo Clin Proc 95:319–327 https://doi.org/10.1016/j.mayocp.2019.08.005
8. Patel MR, Peterson ED, Dai D et al (2010) Low diagnostic yield of elective coronary angiography. N Engl J Med 362:886–895 https://doi.org/10.1056/NEJMoa0907272
9. Lipton MJ, Bogaert J, Boxt LM, Reba RC (2002) Imaging of ischemic heart disease. Eur Radiol 12:1061–1080 https://doi.org/10.1007/s003300101131
10. Maresca D, Correia M, Villemain O et al (2018) Noninvasive imaging of the coronary vasculature using ultrafast ultrasound. JACC Cardiovasc Imaging 11:798–808 https://doi.org/10.1016/j.jcmg.2017.05.021
11. Willemink MJ, Persson M, Pourmorteza A, Pelc NJ, Fleischmann D (2018) Photon-counting CT: technical principles and clinical prospects. Radiology 289:293–312 https://doi.org/10.1148/radiol.2018172656
12. Camici PG, d'Amati G, Rimoldi O (2015) Coronary microvascular dysfunction: mechanisms and functional assessment. Nat Rev Cardiol 12:48–62 https://doi.org/10.1038/nrcardio.2014.160
13. van de Hoef TP, Siebes M, Spaan JA, Piek JJ (2015) Fundamentals in clinical coronary physiology: why coronary flow is more important than coronary pressure. Eur Heart J 36:3312–3319a https://doi.org/10.1093/eurheartj/ehv235

Willemink *et al. European Radiology Experimental*   (2021) 5:12

Page 12 of 14

14. Cikes M, Tong L, Sutherland GR, D'Hooge J (2014) Ultrafast cardiac ultrasound imaging: technical principles, applications, and clinical benefits. JACC Cardiovasc Imaging 7:812–823 https://doi.org/10.1016/j.jcmg.2014.06.004

15. Holbrook M, Clark DP, Badea CT (2018) Low-dose 4D cardiac imaging in small animals using dual source micro-CT. Phys Med Biol 63:025009 https://doi.org/10.1088/1361-6560/aa9b45

16. Goldstein T, Osher S (2009) The split Bregman method for L1-regularized problems. SIAM Journal on Imaging Sciences 2:323–343 https://doi.org/10.1137/080725891

17. Le Quang K, Bouchareb R, Lachance D et al (2014) Early development of calcific aortic valve disease and left ventricular hypertrophy in a mouse model of combined dyslipidemia and type 2 diabetes mellitus. Arterioscler Thromb Vasc Biol 34:2283–2291 https://doi.org/10.1161/ATVBAHA.114.304205

18. Wait JM, Tomita H, Burk LM et al (2013) Detection of aortic arch calcification in apolipoprotein E-null mice using carbon nanotube-based micro-CT system. J Am Heart Assoc 2:e003358 https://doi.org/10.1161/JAHA.112.003358

19. Pai VM, Kozlowski M, Donahue D et al (2012) Coronary artery wall imaging in mice using osmium tetroxide and micro-computed tomography (micro-CT). J Anat 220:514–524 https://doi.org/10.1111/j.1469-7580.2012.01483.x

20. Cao G, Burk LM, Lee YZ et al (2010) Prospective-gated cardiac micro-CT imaging of free-breathing mice using carbon nanotube field emission x-ray. Med Phys 37:5306–5312 https://doi.org/10.1118/1.3491806

21. Martinez HG, Prajapati SI, Estrada CA et al (2009) Images in cardiovascular medicine: microscopic computed tomography-based virtual histology for visualization and morphometry of atherosclerosis in diabetic apolipoprotein E mutant mice. Circulation 120:821–822 https://doi.org/10.1161/CIRCULATIONAHA.108.829531

22. Sangaralingham SJ, Ritman EL, McKie PM et al (2012) Cardiac micro-computed tomography imaging of the aging coronary vasculature. Circ Cardiovasc Imaging 5:518–524 https://doi.org/10.1161/CIRCIMAGING.112.973057

23. Schambach SJ, Bag S, Groden C, Schilling L, Brockmann MA (2010) Vascular imaging in small rodents using micro-CT. Methods 50:26–35 https://doi.org/10.1016/j.ymeth.2009.09.003

24. Badea CT, Hedlund LW, Cook J, Berridge BR, Johnson GA (2011) Micro-CT imaging assessment of dobutamine-induced cardiac stress in rats. J Pharmacol Toxicol Methods 63:24–29 https://doi.org/10.1016/j.vascn.2010.04.002

25. Ashton JR, Befera N, Clark D et al (2014) Anatomical and functional imaging of myocardial infarction in mice using micro-CT and eXIA 160 contrast agent. Contrast Media Mol Imaging 9:161–168 https://doi.org/10.1002/cmmi.1557

26. van Deel E, Ridwan Y, van Vliet JN, Belenkov S, Essers J (2016) In vivo quantitative assessment of myocardial structure, function, perfusion and viability using cardiac micro-computed tomography. J Vis Exp. https://doi.org/10.3791/53603

27. Brenner DJ, Hall EJ (2007) Computed tomography--an increasing source of radiation exposure. N Engl J Med 357:2277–2284 https://doi.org/10.1056/NEJMra072149

28. Sawall S, Franke D, Kirchherr A et al (2017) In vivo quantification of myocardial infarction in mice using micro-CT and a novel blood pool agent. Contrast Media Mol Imaging 2017:2617047 https://doi.org/10.1155/2017/2617047

29. Krauss B, Grant KL, Schmidt BT, Flohr TG (2015) The importance of spectral separation: an assessment of dual-energy spectral separation for quantitative ability and dose efficiency. Invest Radiol 50:114–118 https://doi.org/10.1097/RLI.0000000000000109

30. Sabarudin A, Siong TW, Chin AW, Hoong NK, Karim MKA (2019) A comparison study of radiation effective dose in ECG-gated coronary CT angiography and calcium scoring examinations performed with a dual-source CT scanner. Sci Rep 9:4374 https://doi.org/10.1038/s41598-019-40758-5

31. Symons R, Sandfort V, Mallek M, Ulzheimer S, Pourmorteza A (2019) Coronary artery calcium scoring with photon-counting CT: first in vivo human experience. Int J Cardiovasc Imaging 35:733–739 https://doi.org/10.1007/s10554-018-1499-6

32. Kappler SHT, Göderer E, Kreisler B, Niederloehner D, Stierstorfer K, Flohr T (2012) First results from a hybrid prototype CT scanner for exploring benefits of quantum-counting in clinical CT. Physics of Medical Imaging Progress in Biomedical Optics and Imaging - Proceedings of SPIE:11 https://doi.org/10.1117/12.911295

33. Pourmorteza A, Symons R, Reich DS et al (2017) Photon-counting CT of the brain: in vivo human results and image-quality assessment. AJNR Am J Neuroradiol 38:2257–2263 https://doi.org/10.3174/ajnr.A5402

34. Symons R, Pourmorteza A, Sandfort V et al (2017) Feasibility of dose-reduced chest CT with photon-counting detectors: initial results in humans. Radiology 285:980–989 https://doi.org/10.1148/radiol.2017162587

35. Gutjahr R, Halaweish AF, Yu Z et al (2016) Human imaging with photon counting-based computed tomography at clinical dose levels: contrast-to-noise ratio and cadaver studies. Invest Radiol 51:421–429 https://doi.org/10.1097/RLI.0000000000000251

36. Symons R, De Bruecker Y, Roosen J et al (2018) Quarter-millimeter spectral coronary stent imaging with photon-counting CT: initial experience. J Cardiovasc Comput Tomogr 12:509–515 https://doi.org/10.1016/j.jcct.2018.10.008

37. Mannil M, Hickethier T, von Spiczak J et al (2018) Photon-counting CT: high-resolution imaging of coronary stents. Invest Radiol 53:143–149 https://doi.org/10.1097/RLI.0000000000000420

38. Symons R, Reich DS, Bagheri M et al (2018) Photon-counting computed tomography for vascular imaging of the head and neck: first in vivo human results. Invest Radiol 53:135–142 https://doi.org/10.1097/RLI.0000000000000418

39. Yu Z, Leng S, Jorgensen SM et al (2016) Evaluation of conventional imaging performance in a research whole-body CT system with a photon-counting detector array. Phys Med Biol 61:1572–1595 https://doi.org/10.1088/0031-9155/61/4/1572

40. Cormode DP, Roessl E, Thran A et al (2010) Atherosclerotic plaque composition: analysis with multicolor CT and targeted gold nanoparticles. Radiology 256:774–782 https://doi.org/10.1148/radiol.10092473

41. Symons R, Cork TE, Lakshmanan MN et al (2017) Dual-contrast agent photon-counting computed tomography of the heart: initial experience. Int J Cardiovasc Imaging 33:1253–1261 https://doi.org/10.1007/s10554-017-1104-4

42. Willemink MJ, van der Werf NR, Nieman K, Greuter MJW, Koweek LM, Fleischmann D (2018) Coronary artery calcium: a technical argument for a new scoring method. J Cardiovasc Comput Tomogr. https://doi.org/10.1016/j.jcct.2018.10.014

43. Bornefalk H, Danielsson M (2010) Photon-counting spectral computed tomography using silicon strip detectors: a feasibility study. Phys Med Biol 55:1999–2022 https://doi.org/10.1088/0031-9155/55/7/014

44. Persson M, Huber B, Karlsson S et al (2014) Energy-resolved CT imaging with a photon-counting silicon-strip detector. Phys Med Biol 59:6709–6727 https://doi.org/10.1088/0022-3727/59/22/6709

45. Ronaldson JP, Zainon R, Scott NJ et al (2012) Toward quantifying the composition of soft tissues by spectral CT with Medipix3. Med Phys 39:6847–6857 https://doi.org/10.1118/1.4760773

46. Ibanez B, Aletras AH, Arai AE et al (2019) Cardiac MRI endpoints in myocardial infarction experimental and clinical trials: JACC Scientific Expert Panel. J Am Coll Cardiol 74:238–256 https://doi.org/10.1016/j.jacc.2019.05.024

47. Sosnovik DE, Nahrendorf M, Panizzi P et al (2009) Molecular MRI detects low levels of cardiomyocyte apoptosis in a transgenic model of chronic heart failure. Circ Cardiovasc Imaging 2:468–475 https://doi.org/10.1161/CIRCIMAGING.109.863779

48. Brooks PC, Clark RA, Cheresh DA (1994) Requirement of vascular integrin alphavbeta3 for angiogenesis. Science 264:569-571 https://doi.org/10.1126/science.7512751

49. Makowski MR, Ebersberger U, Nekolla S, Schwaiger M (2008) In vivo molecular imaging of angiogenesis, targeting alphavbeta3 integrin expression, in a patient after acute myocardial infarction. Eur Heart J 29:2201 https://doi.org/10.1093/eurheartj/ehn129

50. Higuchi T, Bengel FM, Seidl S et al (2008) Assessment of alphavbeta3 integrin expression after myocardial infarction by positron emission tomography. Cardiovasc Res 78:395–403 https://doi.org/10.1093/cvr/cvn033

51. Lavin B, Protti A, Lorrio S et al (2018) MRI with gadofosveset: a potential marker for permeability in myocardial infarction. Atherosclerosis 275:400–408 https://doi.org/10.1016/j.atherosclerosis.2018.04.024

52. Mizuno T, Yau TM, Weisel RD, Kiani CG, Li RK (2005) Elastin stabilizes an infarct and preserves ventricular function. Circulation 112:I81–I88 https://doi.org/10.1161/01.CIRCULATIONAHA.105.523795

53. Protti A, Lavin B, Dong X et al (2015) Assessment of myocardial remodeling using an eastin/tropoelastin specific agent with high field magnetic resonance imaging (MRI). J Am Heart Assoc 4:e001851 https://doi.org/10.1161/JAHA.115.001851

54. Wildgruber M, Bielicki I, Aichler M et al (2014) Assessment of myocardial infarction and postinfarction scar remodeling with an elastin-specific magnetic resonance agent. Circ Cardiovasc Imaging 7:321–329 https://doi.org/10.1161/CIRCIMAGING.113.001270

55. Phinikaridou A, Lacerda S, Lavin B et al (2018) Tropoelastin: a novel marker for plaque progression and instability. Circ Cardiovasc Imaging 11 (8). https://doi.org/10.1161/CIRCIMAGING.117.007303

56. Zhuang H, Codreanu I (2015) Growing applications of FDG PET-CT imaging in non-oncologic conditions. J Biomed Res 29:189–202 https://doi.org/10.7555/JBR.29.20140081

57. Thackeray JT, Bankstahl JP, Wang Y, Wollert KC, Bengel FM (2015) Clinically relevant strategies for lowering cardiomyocyte glucose uptake for 18F-FDG imaging of myocardial inflammation in mice. Eur J Nucl Med Mol Imaging 42:771–780 https://doi.org/10.1007/s00259-014-2956-7

58. Tahara N, Mukherjee J, de Haas HJ et al (2014) 2-deoxy-2-[18F]fluoro-D-mannose positron emission tomography imaging in atherosclerosis. Nat Med 20:215–219 https://doi.org/10.1038/nm.3437

59. Hofman MS, Lau WF, Hicks RJ (2015) Somatostatin receptor imaging with 68Ga DOTATATE PET/CT: clinical utility, normal patterns, pearls, and pitfalls in interpretation. Radiographics 35:500–516 https://doi.org/10.1148/rg.352140164

60. Lapa C, Reiter T, Li X et al (2015) Imaging of myocardial inflammation with somatostatin receptor based PET/CT - a comparison to cardiac MRI. Int J Cardiol 194:44–49 https://doi.org/10.1016/j.ijcard.2015.05.073

61. Thackeray JT, Derlin T, Haghikia A et al (2015) Molecular imaging of the chemokine receptor CXCR4 after acute myocardial infarction. JACC Cardiovasc Imaging 8:1417–1426 https://doi.org/10.1016/j.jcmg.2015.09.008

62. Lapa C, Reiter T, Werner RA et al (2015) [(68)Ga]Pentixafor-PET/CT for imaging of chemokine receptor 4 expression after myocardial infarction. JACC Cardiovasc Imaging 8:1466–1468 https://doi.org/10.1016/j.jcmg.2015.09.007

63. Thackeray JT, Bankstahl JP, Wang Y, Wollert KC, Bengel FM (2016) Targeting amino acid metabolism for molecular imaging of inflammation early after myocardial infarction. Theranostics 6:1768–1779 https://doi.org/10.7150/thno.15929

64. Morooka M, Kubota K, Kadowaki H et al (2009) 11C-methionine PET of acute myocardial infarction. J Nucl Med 50 (8):1283-1287. https://doi.org/10.2967/jnumed.108.061341

65. Simonetti OP, Ahmad R (2017) Low-field cardiac magnetic resonance imaging: a compelling case for cardiac magnetic resonance's future. Circ Cardiovasc Imaging 10 https://doi.org/10.1161/CIRCIMAGING.117.005446

66. Wen H, Denison TJ, Singerman RW, Balaban RS (1997) The intrinsic signal-to-noise ratio in human cardiac imaging at 1.5, 3, and 4 T. J Magn Reson 125:65–71 https://doi.org/10.1006/jmre.1996.1072

67. Rajiah P, Bolen MA (2014) Cardiovascular MR imaging at 3 T: opportunities, challenges, and solutions. Radiographics 34:1612–1635 https://doi.org/10.1148/rg.346140048

68. Dietrich O, Reiser MF, Schoenberg SO (2008) Artifacts in 3-T MRI: physical background and reduction strategies. Eur J Radiol 65:29–35 https://doi.org/10.1016/j.ejrad.2007.11.005

69. Hamilton-Craig C, Stäb D, O'Brien K, Galloway G, Barth M (2018) 7-Tesla cardiac magnetic resonance imaging with electrocardiogram gating despite magneto-hydrodynamic effect in healthy volunteers. Heart Lung Circ 27:S205

70. Zhang Y, Xu Y, Wang L et al (2017) Quantitative assessment of salvaged myocardial zone and intramyocardial hemorrhage using non-contrast faster T2 mapping in a rat model by 7T MRI. Exp Ther Med 14:3425–3432 https://doi.org/10.3892/etm.2017.4967

71. Spath NB, Lilburn DML, Gray GA et al (2018) Manganese-enhanced T1 mapping in the myocardium of normal and infarcted hearts. Contrast Media Mol Imaging 2018:9641527 https://doi.org/10.1155/2018/9641527

72. Lohofer F, Hoffmann L, Buchholz R et al (2018) Molecular imaging of myocardial infarction with Gadofluorine P - a combined magnetic resonance and mass spectrometry imaging approach. Heliyon 4:e00606 https://doi.org/10.1016/j.heliyon.2018.e00606

73. Wang L, Chen Y, Zhang B et al (2018) Self-gated late gadolinium enhancement at 7T to image rats with reperfused acute myocardial infarction. Korean J Radiol 19:247–255 https://doi.org/10.3348/kjr.2018.19.2.247

74. Frauenrath T, Hezel F, Renz W et al (2010) Acoustic cardiac triggering: a practical solution for synchronization and gating of cardiovascular magnetic resonance at 7 Tesla. J Cardiovasc Magn Reson 12:67 https://doi.org/10.1186/1532-429X-12-67

75. von Knobelsdorff-Brenkenhoff F, Frauenrath T, Prothmann M et al (2010) Cardiac chamber quantification using magnetic resonance imaging at 7 Tesla--a pilot study. Eur Radiol 20:2844–2852 https://doi.org/10.1007/s00330-010-1888-2

76. Hezel F, Thalhammer C, Waiczies S, Schulz-Menger J, Niendorf T (2012) High spatial resolution and temporally resolved T2* mapping of normal human myocardium at 7.0 Tesla: an ultrahigh field magnetic resonance feasibility study. PLoS One 7:e52324 https://doi.org/10.1371/journal.pone.0052324

77. Prothmann M, von Knobelsdorff-Brenkenhoff F, Topper A et al (2016) High spatial resolution cardiovascular magnetic resonance at 7.0 Tesla in patients with hypertrophic cardiomyopathy - first experiences: lesson learned from 7.0 Tesla. PLoS One 11:e0148066 https://doi.org/10.1371/journal.pone.0148066

78. Pesapane F, Codari M, Sardanelli F (2018) Artificial intelligence in medical imaging: threat or opportunity? Radiologists again at the forefront of innovation in medicine. Eur Radiol Exp 2:35 https://doi.org/10.1186/s41747-018-0061-6

79. Retson TA, Besser AH, Sall S, Golden D, Hsiao A (2019) Machine learning and deep neural networks in thoracic and cardiovascular imaging. J Thorac Imaging 34:192–201 https://doi.org/10.1097/RTI.0000000000000385

80. Tatsugami F, Higaki T, Nakamura Y et al (2019) Deep learning-based image restoration algorithm for coronary CT angiography. Eur Radiol 29:5322–5329 https://doi.org/10.1007/s00330-019-06183-y

81. Albrecht MH, Varga-Szemes A, Schoepf UJ et al (2019) Diagnostic accuracy of noncontrast self-navigated free-breathing MR angiography versus CT angiography: a prospective study in pediatric patients with suspected anomalous coronary arteries. Acad Radiol 26:1309–1317 https://doi.org/10.1016/j.acra.2018.12.010

82. Chen H, Zhang Y, Chen Y et al (2018) LEARN: Learned Experts' Assessment-Based Reconstruction Network for sparse-data CT. IEEE Trans Med Imaging 37:1333–1347 https://doi.org/10.1109/TMI.2018.2805692

83. Chen H, Zhang Y, Kalra MK et al (2017) Low-dose CT with a residual encoder-decoder convolutional neural network. IEEE Trans Med Imaging 36:2524–2535 https://doi.org/10.1109/TMI.2017.2715284

84. Zhu G, Jiang B, Tong L, Xie Y, Zaharchuk G, Wintermark M (2019) Applications of deep learning to neuro-imaging techniques. Front Neurol 10:869 https://doi.org/10.3389/fneur.2019.00869

85. Zreik M, Lessmann N, van Hamersvelt RW et al (2018) Deep learning analysis of the myocardium in coronary CT angiography for identification of patients with functionally significant coronary artery stenosis. Med Image Anal 44:72–85 https://doi.org/10.1016/j.media.2017.11.008

86. van Hamersvelt RW, Zreik M, Voskuil M, Viergever MA, Isgum I, Leiner T (2019) Deep learning analysis of left ventricular myocardium in CT angiographic intermediate-degree coronary stenosis improves the diagnostic accuracy for identification of functionally significant stenosis. Eur Radiol 29:2350–2359 https://doi.org/10.1007/s00330-018-5822-3

87. Xu C, Xu L, Gao Z et al (2017) Direct detection of pixel-level myocardial infarction areas via a deep-learning algorithm. In: Descoteaux M, Maier-Hein L, Franz A, Jannin P, Collins DL, Duchesne S (eds) Medical image computing and computer assisted intervention − MICCAI 2017. Springer International Publishing, Cham, pp 240–249

88. Zhang N, Yang G, Gao Z et al (2019) Deep learning for diagnosis of chronic myocardial infarction on nonenhanced cardiac cine MRI. Radiology 291:606–617 https://doi.org/10.1148/radiol.2019182304

89. Gillies RJ, Kinahan PE, Hricak H (2016) Radiomics: images are more than pictures, they are data. Radiology 278:563–577 https://doi.org/10.1148/radiol.2015151169

90. Kolossvary M, Kellermayer M, Merkely B, Maurovich-Horvat P (2018) Cardiac computed tomography radiomics: a comprehensive review on radiomic techniques. J Thorac Imaging 33:26–34 https://doi.org/10.1097/RTI.0000000000000268

91. Lambin P, Leijenaar RTH, Deist TM et al (2017) Radiomics: the bridge between medical imaging and personalized medicine. Nat Rev Clin Oncol 14:749–762 https://doi.org/10.1038/nrclinonc.2017.141

92. Lambin P, Rios-Velazquez E, Leijenaar R et al (2012) Radiomics: extracting more information from medical images using advanced feature analysis. Eur J Cancer 48:441–446 https://doi.org/10.1016/j.ejca.2011.11.036

93. Mannil M, von Spiczak J, Manka R, Alkadhi H (2018) Texture analysis and machine learning for detecting myocardial infarction in noncontrast low-dose computed tomography: unveiling the invisible. Invest Radiol 53:338–343 https://doi.org/10.1097/RLI.0000000000000448

Willemink *et al. European Radiology Experimental*   (2021) 5:12

Page 14 of 14

94. Baessler B, Mannil M, Oebel S, Maintz D, Alkadhi H, Manka R (2018) Subacute and chronic left ventricular myocardial scar: accuracy of texture analysis on nonenhanced cine MR images. Radiology 286:103–112 https://doi.org/10.1148/radiol.2017170213

95. Larroza A, Lopez-Lereu MP, Monmeneu JV et al (2018) Texture analysis of cardiac cine magnetic resonance imaging to detect nonviable segments in patients with chronic myocardial infarction. Med Phys 45:1471–1480 https://doi.org/10.1002/mp.12783

96. Larroza A, Materka A, Lopez-Lereu MP, Monmeneu JV, Bodi V, Moratal D (2017) Differentiation between acute and chronic myocardial infarction by means of texture analysis of late gadolinium enhancement and cine cardiac magnetic resonance imaging. Eur J Radiol 92:78–83 https://doi.org/10.1016/j.ejrad.2017.04.024

97. Kotu LP, Engan K, Borhani R et al (2015) Cardiac magnetic resonance image-based classification of the risk of arrhythmias in post-myocardial infarction patients. Artif Intell Med 64:205–215 https://doi.org/10.1016/j.artmed.2015.06.001

98. Monti CB, Codari M, van Assen M, De Cecco CN, Vliegenthart R (2020) Machine learning and deep neural networks applications in computed tomography for coronary artery disease and myocardial perfusion. J Thorac Imaging 35:S58–S65 https://doi.org/10.1097/RTI.0000000000000490

99. Litjens G, Ciompi F, Wolterink JM et al (2019) State-of-the-art deep learning in cardiovascular image analysis. JACC Cardiovasc Imaging 12:1549–1565 https://doi.org/10.1016/j.jcmg.2019.06.009

100. Oikonomou EK, Siddique M, Antoniades C (2020) Artificial intelligence in medical imaging: a radiomic guide to precision phenotyping of cardiovascular disease. Cardiovasc Res. https://doi.org/10.1093/cvr/cvaa021

101. Baselli G, Codari M, Sardanelli F (2020) Opening the black box of machine learning in radiology: Can the proximity of annotated cases be a way? Eur Radiol Exp 4:30 https://doi.org/10.1186/s41747-020-00159-0

Publisher's Note